Letter

Perovskite Nanocrystals as a Color Converter for Visible Light Communication

Ibrahim Dursun, Chao Shen, Manas R Parida, Jun Pan, Smritakshi P. Sarmah, Davide Priante, Noktan Alyami, Jiakai Liu, Makhsud I. Saidaminov, Mohd S. Alias, Ahmed L. Abdelhady, Tien Khee Ng, Omar F. Mohammed, Boon S. Ooi, and Osman M. Bakr

ACS Photonics, **Just Accepted Manuscript** • DOI: 10.1021/acsphotonics.6b00187 • Publication Date (Web): 31 May 2016

ACS Photonics is published by the American Chemical Society. 1155 Sixteenth Street N.W., Washington, DC 20036

Perovskite Nanocrystals as a Color Converter for Visible Light Communication

Ibrahim Dursun[1+], Chao Shen[2+], Manas R. Parida[1], Jun Pan[1], Smritakshi P. Sarmah[1], Davide Priante[2], Noktan Alyami[1], Jiakai Liu[1], Makhsud I. Saidaminov[1], Mohd S. Alias[2], Ahmed L. Abdelhady[1], Tien Khee Ng[2], Omar F. Mohammed[1], Boon S. Ooi[2*] and Osman M. Bakr[1*]

[1] Solar and Photovoltaics Engineering Research Center, King Abdullah University of Science and Technology (KAUST), Thuwal 23955-6900, Kingdom of Saudi Arabia

[2] Photonics Laboratory, Computer, Electrical, and Mathematical Sciences and Engineering (CEMSE), King Abdullah University of Science and Technology (KAUST), Thuwal 23955-6900, Kingdom of Saudi Arabia

ABSTRACT

Visible light communication (VLC) is an emerging technology that uses light-emitting diodes (LEDs) or laser diodes for simultaneous illumination and data communication. This technology is envisioned to be a major part of the solution to the current bottlenecks in data and wireless communication. However, the conventional lighting phosphors that are typically integrated with LEDs have limited modulation bandwidth and thus cannot provide the bandwidth required to realize the potential of VLC. In this work, we present a promising light converter for VLC by designing solution-processed $CsPbBr_3$ perovskite nanocrystals (NCs) with a conventional red phosphor. The fabricated $CsPbBr_3$ NCs phosphor-based white light converter exhibits an unprecedented modulation bandwidth of 491 MHz, which is ~ 40 times greater than that of conventional phosphors, and the capability to transmit a high data rate of up to 2 Gbit/s. Moreover, this perovskite enhanced white light source combines ultrafast response characteristics with a high color rendering index of 89 and a low correlated color temperature of 3236 K, thereby enabling dual VLC and solid-state lighting functionalities.

Keywords: perovskite, phosphors, transient absorption spectroscopy, visible light communication and solid-state lighting

Data and wireless communications support much of the economic and social structures underlying our daily lives. Over the next decade, the demand for communications systems and data transfer, especially wireless technologies, is expected to grow at an exponential rate. Existing radio frequency (RF) and microwave wireless technologies cannot keep up with this surging demand because of their crowded spectra and limited bandwidth. Expanding the wireless communications window by using white light provides a new pathway for uninhibited growth in data communications and consumption. Light-emitting diodes (LEDs) can be utilized as light sources not only for illumination but also for data transmission; the latter application is referred to as visible light communication (VLC) [1-4]. VLC has many advantages compared with lower-frequency communications approaches (including Wi-Fi and Bluetooth), such as energy efficiency, an unregulated communication spectrum, environmental friendliness, greater security, and no RF interferences [2, 5, 6].

A typical white light source in a VLC system is made of a blue-emitting LED or a laser diode (LD) with phosphors partially converting blue light into green, yellow and/or red emission[7]. The conventional phosphor for white LED (WLED) illumination, yttrium aluminum garnet (YAG) phosphor $Y_{3-x}Al_5O_{12}:xCe^{3+}$ (YAG:Ce)[8], has a critical limitation for VLC applications due to the slow phosphor conversion process caused by the long excited state lifetimes[3], on the order of microseconds. As a result, the phosphor-associated bandwidth limit is a few (~3-12) megahertz (MHz) in unfiltered VLC systems[3, 9]. To overcome this VLC bottleneck, organic materials, such as BODIPY, MEH-PPV and BBEHP-PPV, have been presented as potential candidates for white light VLC color converters because of their visible light emission, high photoluminescence quantum yield (PLQY), direct radiative recombination and ease of integration with nitride-based semiconductors[9-11]. However, they still suffer from their long excited state lifetimes, thus limiting their modulation bandwidth frequencies to the range of ~ 40-200 MHz. Therefore, the development of a light converter phosphor material with a fast decay and a high-efficiency (i.e. short radiative lifetime and high brightness) remains the major challenge for VLC and solid state lighting (SSL) applications.

Recently, lead halide perovskites (ABX_3; where A = $CH_3NH_3^+$, Cs^+ or $HC(NH_2)_2^+$; B = Pb^{2+}; X = Br^-, I^- and/or Cl^-) have been extensively used for optoelectronic devices, such as photovoltaic cells[12], lasers[13-15], LEDs[16] and photodetectors[17, 18]. The primary advantages of these perovskites include long-range charge transport [19, 20], tunable emission in the visible spectrum, low cost, and facile processability at relatively low temperatures. In particular, nanocrystals (NCs) of $CsPbBr_3$ perovskites exhibit high PLQY (≥ 70%) [21-23] and a relatively short PL lifetime[21]. These characteristics make perovskites attractive for displays [24] and white light emission[25-27]. Here, we investigate the fast and predominantly radiative recombination characteristics of $CsPbBr_3$ perovskite NCs as a light converter for VLC in addition to the generation of white light for SSL. A record light converter-associated modulation bandwidth of 491 MHz was measured in our system, which is significantly greater than those of conventional nitride-based phosphors (3-12 MHz) and organic polymers (200 MHz)[10]. The light source generates bright warm white light with high CRI – as much as 89 – and a correlated color temperature (CCT) of greater than 3200 K. To the best of our knowledge, this work reports the first VLC system with solution-processed perovskite NCs. This work breaks the bandwidth limitation barrier of phosphor-converted white light VLC systems and showcases a novel utilization of $CsPbBr_3$ perovskite NCs as efficient and effective alternative phosphor materials for VLC and SSL applications simultaneously.

We synthesized $CsPbBr_3$ perovskite NCs via a modified hot-injection method similar to that presented in previous work[28] (see the experimental section). The NCs were characterized by high resolution transmission electron microscopy (HRTEM) (Figures S1), which revealed uniform cubic shaped NCs with an average size of 8.3 ± 0.8 nm. The X-ray diffraction (XRD) pattern of the NCs exhibited the cubic $CsPbBr_3$ phase (see Figure S2). Figure 1a inset shows the absorption and photoluminescence (PL) spectra of the NCs dispersed in toluene. As can be seen, the absorption spectrum of the $CsPbBr_3$ NCs does not exhibit any spectral features at wavelengths longer than ~520 nm, which is consistent with previous reports [21, 29, 30]. The NCs exhibit a sharp PL emission peak at 512 nm with a narrow full width at half maximum (FWHM) of 22 nm.

Time-resolved laser spectroscopy has proven to be a critical part of studying excited state dynamics[31-33]. Here, to study the carrier dynamics of these $CsPbBr_3$ NCs, we performed femto-nanoseconds transient absorption (fs-ns- TA) experiments (experimental setup detailed elsewhere [34, 35]) and time-resolved PL measurements and the results are presented in Figure 1. The ns- TA measurement was recorded following laser pulse excitation at 350 nm with a pump fluence of 9 μJ/cm^2. In this TA experiment, we followed the ground-state bleach (GSB) recovery to monitor the charge recombination dynamics, as shown in Figure 1a. The GSB observed at approximately 505 nm, which corresponds to the steady-state absorption spectrum, reveals a full recovery in a 30-ns time window with a time constant of 6.4 ns (shown in Figure 1b). Because of the low pump intensity for photo-excitation, Auger recombination due to carrier multiplication generated by multi-photon absorption is not appreciable[36]. To also confirm that a multiple exciton generation process is not dominant in the observed dynamics, we performed the TA experiments at two different pump fluencies (9 and 18 μJ/cm^2) and almost identical kinetics are recorded as shown in Figure 1b.

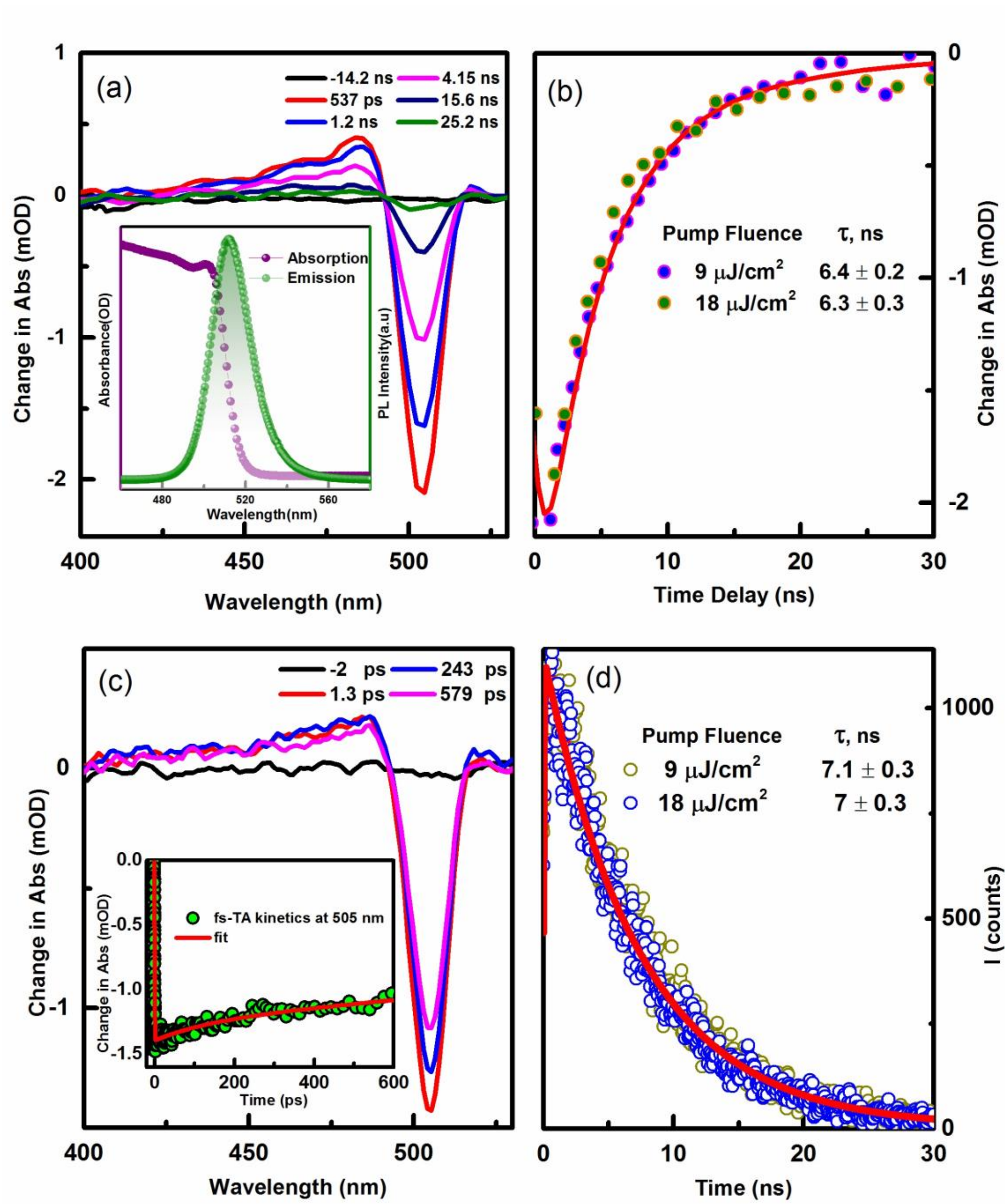

Figure 1. Carrier dynamics in $CsPbBr_3$. (a) ns-TA spectra of $CsPbBr_3$ NCs in toluene at the indicated delay times. Inset: (a) Absorption (pink) and PL (olive) spectra of $CsPbBr_3$ NCs in toluene. (b) Transient traces corresponding to the GSB from the ns-TA spectra of $CsPbBr_3$ NCs. (c) fs-TA spectra of $CsPbBr_3$ NCs. Inset: kinetics in 0.0-5.5 ns time window. (d) ns-

photoluminescence decay of $CsPbBr_3$ NCs monitored at 515 nm . The solid red lines are the best fits of the kinetic traces.

Additionally, we have performed the fs-TA of $CsPbBr_3$ NCs and the results are shown in Figure 1c. The GSB recovery shows an additional component with a characteristic time constant of 103 ± 40 ps which may be attributed to non-radiation recombination due to surface traps[37, 38]. To further understand the carrier dynamics and the radiative recombination process, we measured the PL lifetime via time-correlated single-photon counting (TCSPC) using a fluorescence up-conversion spectrometer with excitation at 400 nm (Figure 1d). The PL lifetime decay profile was collected at 515 nm. The decay curve can be fitted with a single exponential function with a lifetime of approximately 7.0 ± 0.3 ns. It is worth pointing out that the PL decay of $CsPbBr_3$ NCs with two different excitation fluencies shows a similar decay trend (see Figure 1d), which is consistent with TA data. This short lifetime of about 7 ns is comparable with the reported values for similar sized of $CsPbBr_3$ NCs [21, 39, 40]. We have also observed similar kinetics trend from both solution and film samples of $CsPbBr_3$ NCs in time-resolved experiments shown in Figure S3. Because of their high PLQY of ~ 70 % and short radiative recombination lifetime of 7.0 ± 0.3 ns, $CsPbBr_3$ NCs have promising materials for generating VLC and SSL.

To study the white light generated by utilizing $CsPbBr_3$ NCs as light converters for SSL, a mixture of green-emitting $CsPbBr_3$ NCs phosphor with a red-emitting nitride phosphor (LAM-R-6237, Dalian Luming Group) ($CsPbBr_3$ NCs are drop casted onto red-emitting phosphor to form a film) is excited by a GaN blue-emitting LD (λ = 450 nm) (see Figure 2a inset). Operating at 200 mA, the LD generates a warm white light (CCT = 3236 K) with a CRI value of 89, as calculated after its emission passes through the phosphor mixture. Compared with the warm white LED bulbs available on the market, which have a typical CRI of 70-80, the white light generated herein achieves higher quality emission that is suitable for lighting. Figure 2a, b shows the spectrum and the chromaticity diagram (CIE 1931) coordinates (0.3823, 0.3079) of the generated white light. The CRI value of the $CsPbBr_3$ NCs with red-emitting phosphor is also greater than that reported value of 76 for organic down-converted white VLC transmitters[10]. Our device also shows enhanced performance than commercial WLEDs based on YAG:Ce^{3+} phosphor, which exhibit relatively low CRI (<75) and high CCT (>7765 K)[41]. The device using perovskite NCs phosphor as demonstrated in this work suggests better quality of white light. In comparison, our results present a higher CRI of 89 and a lower CCT of 3236 K, which are essential factors for indoor illuminations[42] and optical display applications[41].

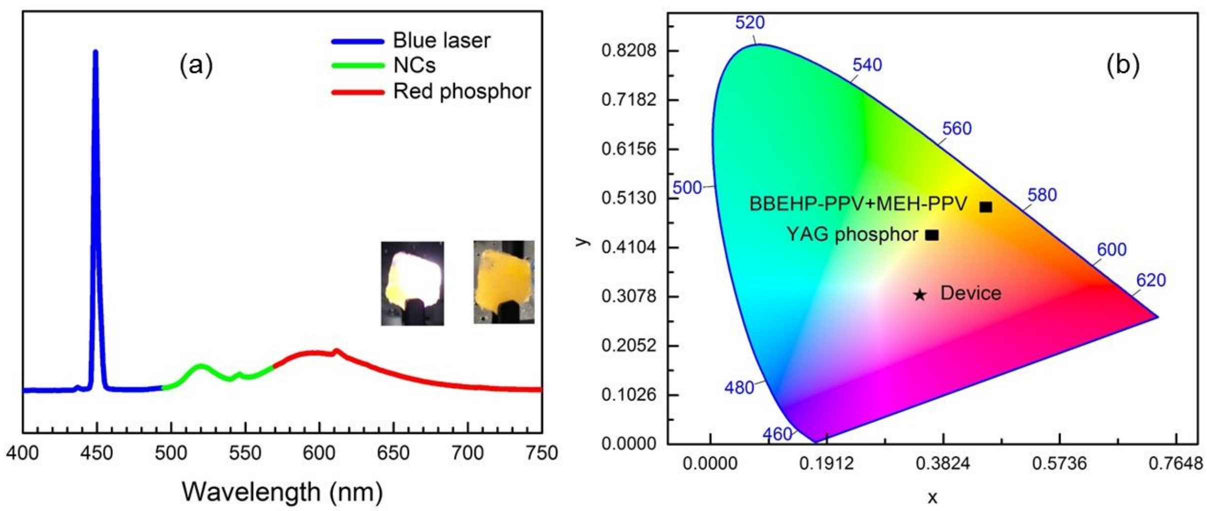

Figure 2. $CsPbBr_3$ NCs for SSL. (a) Spectrum of white light generated using blue laser, green-emitting perovskite NCs and conventional nitride-based red phosphor. Inset: photographs of phosphor with perovskite under ambient light (right) and generated white light under blue laser (left). (b) Generated white light in the CIE 1931 color space (chromaticity coordinates). For a comparison single crystal YAG phosphor[7] and BBEHP-PPV+MEH-PPV (75:25) mixture phosphor[10] are also plotted.

To investigate the modulation bandwidth in $CsPbBr_3$ NCs phosphor-converted white light, we performed a small-signal frequency-response measurement (Figure 3a). A -10 dBm sinusoidal AC modulation signal was superimposed on a DC bias current to drive the LD. Both the laser emission and phosphor converted light are then collected by the photodetector. By sweeping the AC modulation frequency from 10 MHz to 2 GHz, the response of the overall system response including the phosphor-converted lighting system, is measured by comparing the transmitted signal and received signal. The modulation bandwidth of the blue LD (B-LD) was measured without phosphor and optical filters inserted. The frequency response of B-LD + NCs + red-phosphor, NCs + red-phosphor, and red-phosphor only was measured with no optical filter, a 500 nm long-pass filter, and a 550 nm long-pass filter, respectively. Short recombination lifetime is the key parameter for VLC applications because the capacity of a communications channel is related to the bandwidth[43] and lifetime. We posited that due to their desirable carrier recombination lifetimes, $CsPbBr_3$ NCs as light convertors have great potential for high modulation bandwidth devices and could overcome the current data transmission bottleneck in slow response (limited bandwidth) of conventional phosphor-converted WLED. Indeed, we found $CsPbBr_3$ NCs phosphor-converted light exhibits a relatively high bandwidth of 491.4 MHz (Figure 3b), which is significantly greater than those of conventional nitride-based phosphors (~12.4 MHz), organic materials (40-200 MHz) [5, 9, 10], commercial YAG-based phosphors (3-12 MHz) [44, 45] and blue LEDs [46]. In addition to these materials, colloidal quantum dots (CQDs) are also potential wavelength conversion materials for VLC. Leurand et. al. reported that CQDs (core-shell CdSe/ZnS) are capable of generating white light when excited by a 450 nm blue LED, however, the frequency response is considerably low (-3 dB bandwidth of 10 ~ 25 MHz) – as a result of their substantially slower carrier relaxation dynamics[47]. Using the fast-response $CsPbBr_3$ NCs as a phosphor, we also demonstrated the data transmission of phosphor-converted LD-based VLC using an on-off keying (OOK) modulation scheme. The OOK is the basic form of amplitude shift keying modulation scheme for wireless communication, where the presence or absence of carrier wave represents the ones and zeros of digital data, respectively. A pseudorandom binary sequence (PRBS) 2^{10}-1 data-format was used to modulate the laser intensity, thus transmitting data in a wireless manner. The schematic of the data transmission measurement by OOK is illustrated in Figure 3c**.** The $CsPbBr_3$ NCs were deposited on a plastic diffuser to serve as a phosphor. The bit-error-rates (BERs) at variable data rates are demonstrated in Figure 3d, where a BER of 7.4×10^{-5} is measured at 2 Gbit/s. The obtained BER measurement adheres to the forward error correction (FEC) standard (BER ≤ 3.8×10-3). The clear open eye as observed in the eye diagram (inset of Figure 3d) suggests that the CsPbBr3 NCs phosphor-converted LD VLC is capable of transmitting a high data rate of up to 2 Gbit/s. Finally, we have investigated the operational stability of the films in air, without any encapsulation, under continuous blue laser illumination. Despite having no special protecting layer, the films show promising photostability (see Figure S4).

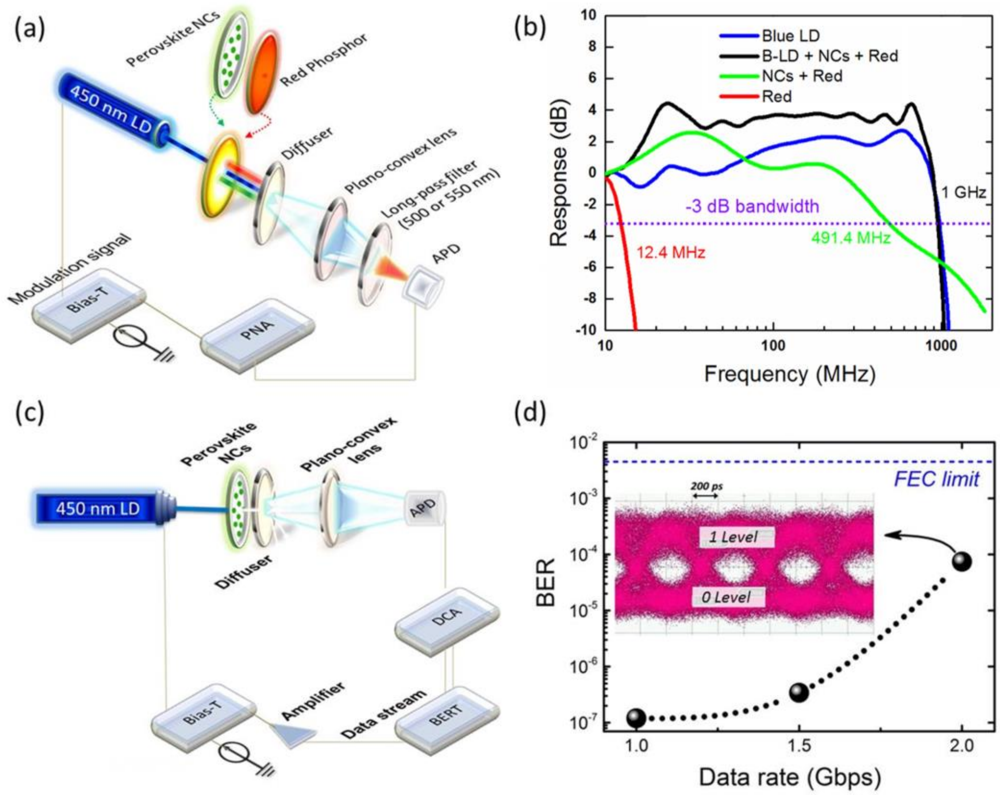

Figure 3. Modulation bandwidth and data transmission measurements using perovskite NCs. (a) Schematic drawing of the small-signal frequency-response measurement setup used to obtain results in (b). (b) Measured frequency response of 1) blue LD, where no phosphor or optical filter presented; 2) laser diode together with phosphor-generated white light, where no optical filter is used; 3) phosphor-converted green and red light, where a 500 nm long-pass filter is used; and 4) phosphor-converted red light, where a 550 nm long-pass filter is mounted. (c) Schematic of the data transmission measurement using an OOK scheme used to obtain results in (d). (d) Bit-error-rates (BERs) at different data rates, whit the forward error correction (FEC) limit labelled. Inset: eye diagram of 2 Gbit/s data rate showing with a clear open eye.

In conclusion, we have demonstrated the $CsPbBr_3$ NCs' potential to serve as fast color converters for VLC and SSL by mixing them with a red-emitting nitride phosphor. The direct radiative recombination and short PL lifetime of $CsPbBr_3$ perovskite NCs enabled us to utilize them as phosphors for dual-function VLC and SSL systems. Because of the short recombination lifetime of $CsPbBr_3$ NCs (relative to conventional phosphor-based materials), the converted white light (with a high CRI of 89 and a low CCT of 3236 K) exhibits an extraordinary modulation bandwidth of 491 MHz, which is 40 times greater than that of conventional phosphors. The fast response and desirable color characteristics of $CsPbBr_3$ NCs as a phosphor material pave the way for a new generation of dual-function systems for VLC and SSL with high brightness and a high Gbit/s data transfer rates. Although Br-based all-inorganic perovskites are known for their stability, we envision that similar to all existing phosphors technologies, further development of the perovskite material as a light converter would entail proper encapsulation[48] and packaging processes to ensure operational reliability throughout the life-span of the lighting device.

EXPERIMENTAL METHOD

Chemicals and materials: 1-Butanol (BuOH, HPLC grade), was purchased from J. T. Baker and Fisher Scientific, respectively. Oleic acid (OA, technical grade 90%), lead bromide ($PbBr_2$, 98+%) and octane (98+%) were purchased from Alpha Aesar. Cesium carbonate (Cs_2CO_3, 99.995%, metal basis), oleylamine (OAm, technical grade 70%), and 1-octadecene (ODE, technical grade 90%) were purchased from Sigma-Aldrich. Toluene (HPLC grade) was purchased from Honeywell Burdick & Jackson. All the chemicals were used as procured without further purification.

Preparation of Cs-oleate: Cs_2CO_3 (0.814 g) along with ODE (40 mL) and OA (2.5 mL) were loaded into a 100 mL 2-neck flask, dried for 1h at 120 °C, and then heated under N_2 at 150 °C until all Cs_2CO_3 reacted with OA. The solution was maintained at 150 °C before injection inorder to avoid solidification of Cs-oleate.

Synthesis of $CsPbBr_3$ NCs: Similar as the previous report[28], ODE (50 mL) and $PbBr_2$ (0.69 g) were loaded into a 250 mL 2-neck round bottomed flask and dried under vacuum for 1h at 120 °C. OAm (5 mL) and OA (5 mL) were then injected at 120 °C under N_2. After complete dissolving of the $PbBr_2$ salt, the temperature was raised to 180 °C and the Cs-oleate solution (4 mL, prepared as described above) was quickly injected. The reaction mixture was cooled in an ice-water bath after 5 seconds.

Selected purification of $CsPbBr_3$ NCs: The crude solution was cooled down with an ice-water bath and transferred to centrifuge tubes directly. After centrifuging at 8000 rpm for 15 min, supernatant was discarded and the precipitate was collected separately. The precipitate was dispersed in toluene for centrifugation at 7000 rpm for 5 min, remove the supernatant and collect the new precipitate for another centrifugation by dispersing in toluene. Then the shining green solution was collect for further experiment.

Characterization: UV-vis absorption spectra were obtained using an absorption spectrophotometer from Ocean Optics. Photoluminescence was tested using an FLS920 dedicated fluorescence spectrometer from Edinburgh Instruments. Quantum yield was measured using an Edinburgh Instruments integrating sphere[49] with an FLS920-s fluorescence spectrometer. Powder X-ray diffraction (XRD) patterns were recorded using Siemens diffractometer with Cu Kα radiation (λ=1.54178 Å).TEM analysis was carried out with a Titan™ TEM (FEI Company) operating at a beam energy of 300 keV and equipped with a Tridiem™ post-column energy filter (Gatan, INC.). The samples were imaged in energy-filtered TEM (EFTEM) mode with a 20 eV energy slit inserted around the zero-energy-loss electrons to acquire high-resolution TEM (HRTEM) micrographs.

Transient absorption spectroscopy measurements: The ns transient absorption spectroscopy measurement was recorded following laser pulse excitation at 350 nm with 9 μJ/cm^2. The ns time-resolved spectra were measured with a pump−probe EOS setup, in which a standard probe reference channel is attached. The fs-TA spectra were measured with Helios setup, in which a white light continuum probe pulse was generated in a 2 mm thick sapphire plate contained in an Ultrafast System LLC spectrometer. In both this arrangement the probe beam is split into two, one travels through sample and the other is sent directly to the reference spectrometer that monitors the fluctuations in the probe beam intensity. The pump beam comes from a Ti:sapphire femtosecond regenerative amplifier operating at 800 nm with 35 fs pulses and a repetition rate of 1 kHz. Spectrally tunable (240−2600 nm) femtosecond pulses generated by an Optical Parametric Amplifier (Light Conversion LTD), as the pump (excitation) in the pump−probe experimental setup (EOS). Time-correlated single photon counting (TCSPC), used for lifetime measurements, was performed using a Halcyone MC multichannel fluorescence upconversion spectrometer.

White light emission experiments: By mixing the green emitting perovskite $CsPbBr_3$ NCs phosphor with red emitting nitride phosphor (LAM-R-6237, Dalian Luming Group), the phosphor is excited by a GaN based blue emitting laser diode (λ = 450 nm). The phosphors converted white light was characterized using GL Spectis 5.0 Touch spectrometer from GL Optics.

Bandwidth Measurement: The setup consisted of a Keithley 2400 source meter as the DC power supply, an Agilent E8361C PNA network analyzer, Picosecond Pulse Labs 5543 bias tee, and Menlo Systems APD 210 high-speed Si avalanche photodetector.

Eye diagram measurements: This experiment involve a GaN-based blue laser diode to pump perovskite NCs on a plastic diffuser as phosphor material. The input signal from the bit error rate tester (BERT, Agilent N4903B J-BERT) was pre-amplified using a 26 dB driver amplifier

(Picosecond 5865, maximum bandwidth 12.5 GHz) and then jointed with a DC bias using a bias-tee before being feed into the LD. The modulated light was received by a 1 GHz APD 210 high-speed Si avalanche photodetector from Menlo Systems. The eye diagrams of received signals were measured by a digital communications analyzer (DCA, Agilent 86100).

ASSOCIATED CONTENT

Supporting Information Available: TEM, XRD, photostability, and supplementary time-resolved optical spectroscopy data of $CsPbBr_3$ NCs.

This material is available free of charge via the Internet at http://pubs.acs.org.

AUTHOR INFORMATION

Corresponding Authors

*E-mails: osman.bakr@kaust.edu.sa and boon.ooi@kaust.edu.sa

[+]These authors contributed equally to this work (I.D. and C.S.).

Notes

The authors declare no competing financial interest.

ACKNOWLEDGEMENTS

The authors acknowledge the financial support of King Abdullah University of Science and Technology (KAUST) and King Abdulaziz City for Science and Technology (KACST), grant No. KACST TIC R2-FP-008.

REFERENCES

1. Burchardt, H.; Serafimovski, N.; Tsonev, D.; Videv, S.; Haas, H. VLC: Beyond point-to-point communication. *IEEE Commun. Mag.* **2014**, 52, 98-105.

2. Elgala, H.; Mesleh, R.; Haas, H.; Pricope, B. In *OFDM Visible Light Wireless Communication Based on White LEDs*, Vehicular Technology Conference, (VTC2007-Spring) IEEE 65th, April **2007**, pp 2185-2189.

3. O'Brien, D.; Zeng, L.; Hoa, L.-M.; Faulkner, G.; Walewski, J. W.; Randel, S. In *Visible light communications: Challenges and possibilities*, Personal, Indoor and Mobile Radio Communications, (PIMRC 2008), IEEE 19th International Symposium, **2008**, pp 1-5.

4. Chun, H.; Chiang, C.-J.; Monkman, A.; O'Brien, D. A Study of Illumination and Communication using Organic Light Emitting Diodes. *J. Lightw. Technol.* **2013**, 31, 3511-3517.

5. Sajjad, M. T.; Manousiadis, P. P.; Orofino, C.; Cortizo-Lacalle, D.; Kanibolotsky, A. L.; Rajbhandari, S.; Amarasinghe, D.; Chun, H.; Faulkner, G.; O'Brien, D. C.; Skabara, P. J.; Turnbull, G. A.; Samuel, I. D. W. Fluorescent Red-Emitting BODIPY Oligofluorene Star-Shaped Molecules as a Color Converter Material for Visible Light Communications. *Adv. Opt. Mater.* **2015**, 3, 536-540.

6. Rajbhandari, S.; Chun, H.; Faulkner, G.; Cameron, K.; Jalajakumari, A. V. N.; Henderson, R.; Tsonev, D.; Ijaz, M.; Chen, Z.; Haas, H.; Xie, E.; McKendry, J. J. D.; Herrnsdorf, J.; Gu, E.; Dawson, M. D.; Brien, D. O. High-Speed Integrated Visible Light Communication System: Device Constraints and Design Considerations. *IEEE J. Sele. Areas in Commun.* **2015**, 33, 1750-1757.

7. Lee, C.; Shen, C.; Oubei, H. M.; Cantore, M.; Janjua, B.; Ng, T. K.; Farrell, R. M.; El-Desouki, M. M.; Speck, J. S.; Nakamura, S.; Ooi, B. S.; DenBaars, S. P. 2 Gbit/s data transmission

from an unfiltered laser-based phosphor-converted white lighting communication system. *Opt. Express* **2015**, 23, 29779-29787.

8. Schubert, E. F.; Gessmann, T.; Kim, J. K. *Light Emitting Diodes*. Willey Online Library, **2005**

9. Hyunchae, C.; Manousiadis, P.; Rajbhandari, S.; Vithanage, D. A.; Faulkner, G.; Tsonev, D.; McKendry, J. J. D.; Videv, S.; Enyuan, X.; Erdan, G.; Dawson, M. D.; Haas, H.; Turnbull, G. A.; Samuel, I. D. W.; O'Brien, D. C. Visible Light Communication Using a Blue GaN µLED and Fluorescent Polymer Color Converter. *IEEE Photonics Technol. Lett.* **2014**, 26, 2035-2038.

10. Sajjad, M. T.; Manousiadis, P. P.; Chun, H.; Vithanage, D. A.; Rajbhandari, S.; Kanibolotsky, A. L.; Faulkner, G.; O'Brien, D.; Skabara, P. J.; Samuel, I. D. W.; Turnbull, G. A. Novel Fast Color-Converter for Visible Light Communication Using a Blend of Conjugated Polymers. *ACS Photonics* **2015**, 2, 194-199.

11. Farinola, G. M.; Ragni, R. Electroluminescent materials for white organic light emitting diodes. *Chem. Soc. Rev.* **2011**, 40, 3467-3482.

12. Liu, M.; Johnston, M. B.; Snaith, H. J. Efficient planar heterojunction perovskite solar cells by vapour deposition. *Nature* **2013**, 501, 395-398.

13. Deschler, F.; Price, M.; Pathak, S.; Klintberg, L. E.; Jarausch, D.-D.; Higler, R.; Hüttner, S.; Leijtens, T.; Stranks, S. D.; Snaith, H. J.; Atatüre, M.; Phillips, R. T.; Friend, R. H. High Photoluminescence Efficiency and Optically Pumped Lasing in Solution-Processed Mixed Halide Perovskite Semiconductors. *J. Phys. Chem. Lett.* **2014**, 5, 1421-1426.

14. Xing, G.; Mathews, N.; Lim, S. S.; Yantara, N.; Liu, X.; Sabba, D.; Grätzel, M.; Mhaisalkar, S.; Sum, T. C. Low-temperature solution-processed wavelength-tunable perovskites for lasing. *Nat. Mater* **2014**, 13, 476-480.

15. Yakunin, S.; Protesescu, L.; Krieg, F.; Bodnarchuk, M. I.; Nedelcu, G.; Humer, M.; De Luca, G.; Fiebig, M.; Heiss, W.; Kovalenko, M. V. Low-threshold amplified spontaneous emission and lasing from colloidal nanocrystals of caesium lead halide perovskites. *Nat. Commun* **2015**, 6.

16. Tan, Z.-K.; Moghaddam, R. S.; Lai, M. L.; Docampo, P.; Higler, R.; Deschler, F.; Price, M.; Sadhanala, A.; Pazos, L. M.; Credgington, D.; Hanusch, F.; Bein, T.; Snaith, H. J.; Friend, R. H. Bright light-emitting diodes based on organometal halide perovskite. *Nat. Nano* **2014**, 9 (9) 687-692.

17. Saidaminov, M. I.; Adinolfi, V.; Comin, R.; Abdelhady, A. L.; Peng, W.; Dursun, I.; Yuan, M.; Hoogland, S.; Sargent, E. H.; Bakr, O. M. Planar-integrated single-crystalline perovskite photodetectors. *Nat. Commun* **2015**, 6, 7586.

18. Dou, L.; Yang, Y.; You, J.; Hong, Z.; Chang, W.-H.; Li, G.; Yang, Y. Solution-processed hybrid perovskite photodetectors with high detectivity. *Nat. Commun* **2014**, 5 5404.

19. Shi, D.; Adinolfi, V.; Comin, R.; Yuan, M.; Alarousu, E.; Buin, A.; Chen, Y.; Hoogland, S.; Rothenberger, A.; Katsiev, K.; Losovyj, Y.; Zhang, X.; Dowben, P. A.; Mohammed, O. F.; Sargent, E. H.; Bakr, O. M. Low trap-state density and long carrier diffusion in organolead trihalide perovskite single crystals. *Science* **2015**, 347, 519-522.

20. Dong, Q.; Fang, Y.; Shao, Y.; Mulligan, P.; Qiu, J.; Cao, L.; Huang, J. Electron-hole diffusion lengths > 175 μm in solution-grown CH3NH3PbI3 single crystals. *Science* **2015**, 347, 967-970.

21. Protesescu, L.; Yakunin, S.; Bodnarchuk, M. I.; Krieg, F.; Caputo, R.; Hendon, C. H.; Yang, R. X.; Walsh, A.; Kovalenko, M. V. Nanocrystals of Cesium Lead Halide Perovskites (CsPbX3, X = Cl, Br, and I): Novel Optoelectronic Materials Showing Bright Emission with Wide Color Gamut. *Nano Lett.* **2015**, 15, 3692-3696.

22. Akkerman, Q. A.; D'Innocenzo, V.; Accornero, S.; Scarpellini, A.; Petrozza, A.; Prato, M.; Manna, L. Tuning the Optical Properties of Cesium Lead Halide Perovskite Nanocrystals by Anion Exchange Reactions. *J. Am. Chem. Soc.* **2015**, 137, 10276-10281.

23. Nedelcu, G.; Protesescu, L.; Yakunin, S.; Bodnarchuk, M. I.; Grotevent, M. J.; Kovalenko, M. V. Fast Anion-Exchange in Highly Luminescent Nanocrystals of Cesium Lead Halide Perovskites (CsPbX3, X = Cl, Br, I). *Nano Lett.* **2015**, 15, 5635-5640.

24. Zhang, F.; Zhong, H.; Chen, C.; Wu, X.-g.; Hu, X.; Huang, H.; Han, J.; Zou, B.; Dong, Y. Brightly Luminescent and Color-Tunable Colloidal CH3NH3PbX3 (X = Br, I, Cl) Quantum Dots: Potential Alternatives for Display Technology. *ACS Nano* **2015**, 9, 4533-4542.

25. Dohner, E. R.; Jaffe, A.; Bradshaw, L. R.; Karunadasa, H. I. Intrinsic White-Light Emission from Layered Hybrid Perovskites. *J. Am. Chem. Soc.* **2014**, 136, 13154-13157.

26. Dohner, E. R.; Hoke, E. T.; Karunadasa, H. I. Self-Assembly of Broadband White-Light Emitters. *J. Am. Chem. Soc.* **2014**, 136, 1718-1721.

27. Pathak, S.; Sakai, N.; Wisnivesky Rocca Rivarola, F.; Stranks, S. D.; Liu, J.; Eperon, G. E.; Ducati, C.; Wojciechowski, K.; Griffiths, J. T.; Haghighirad, A. A.; Pellaroque, A.; Friend, R. H.; Snaith, H. J. Perovskite Crystals for Tunable White Light Emission. *Chem. Mater.* **2015**, 27, 8066-8075.

28. Pan, J.; Sarmah, S. P.; Murali, B.; Dursun, I.; Peng, W.; Parida, M. R.; Liu, J.; Sinatra, L.; Alyami, N.; Zhao, C.; Alarousu, E.; Ng, T. K.; Ooi, B. S.; Bakr, O. M.; Mohammed, O. F. Air-Stable Surface-Passivated Perovskite Quantum Dots for Ultra-Robust, Single- and Two-Photon-Induced Amplified Spontaneous Emission. *J. Phys. Chem. Lett.* **2015**, 5027-5033.

29. Park, Y.-S.; Guo, S.; Makarov, N. S.; Klimov, V. I. Room Temperature Single-Photon Emission from Individual Perovskite Quantum Dots. *ACS Nano* **2015**, 9, 10386-10393.

30. Wang, Y.; Li, X.; Zhao, X.; Xiao, L.; Zeng, H.; Sun, H. Nonlinear Absorption and Low-Threshold Multiphoton Pumped Stimulated Emission from All-Inorganic Perovskite Nanocrystals. *Nano Lett.* **2015**, 16 (1), 448-453.

31. Mohammed, O. F.; Banerji, N.; Lang, B.; Nibbering, E. T. J.; Vauthey, E. Photoinduced Bimolecular Electron Transfer Investigated by Femtosecond Time-Resolved Infrared Spectroscopy. *J. Phys. Chem. A* **2006**, 110, 13676-13680.

32. Mohammed, O. F.; Vauthey, E. Simultaneous Generation of Different Types of Ion Pairs upon Charge-Transfer Excitation of a Donor−Acceptor Complex Revealed by Ultrafast Transient Absorption Spectroscopy. *J. Phys. Chem. A* **2008**, 112, 5804-5809.

33. Aly, S. M.; Goswami, S.; Alsulami, Q. A.; Schanze, K. S.; Mohammed, O. F. Ultrafast Photoinduced Electron Transfer in a π-Conjugated Oligomer/Porphyrin Complex. *J. Phys. Chem. Lett.* **2014**, 5, 3386-3390.

34. Parida, M. R.; Aly, S. M.; Alarousu, E.; Mohammed, O. F. Tunable Photophysical Processes of Porphyrin Macrocycles on the Surface of ZnO Nanoparticles. *J. Phys. Chem. C* **2015**, 119, 2614-2621.

35. Mohammed, O. F.; Xiao, D.; Batista, V. S.; Nibbering, E. T. J. Excited-State Intramolecular Hydrogen Transfer (ESIHT) of 1,8-Dihydroxy-9,10-anthraquinone (DHAQ) Characterized by Ultrafast Electronic and Vibrational Spectroscopy and Computational Modeling. *J. Phys. Chem. A* **2014**, 118, 3090-3099.

36. Wehrenfennig, C.; Eperon, G. E.; Johnston, M. B.; Snaith, H. J.; Herz, L. M. High Charge Carrier Mobilities and Lifetimes in Organolead Trihalide Perovskites. *Adv. Mater.* **2014**, 26, 1584-1589.

37. Wang, Y.; Li, X.; Song, J.; Xiao, L.; Zeng, H.; Sun, H. All-Inorganic Colloidal Perovskite Quantum Dots: A New Class of Lasing Materials with Favorable Characteristics. *Adv. Mater.* **2015**, 27, 7101-7108.

38. Ivanov, S. A.; Achermann, M. Spectral and Dynamic Properties of Excitons and Biexcitons in Type-II Semiconductor Nanocrystals. *ACS Nano* **2010**, 4, 5994-6000.

39. Swarnkar, A.; Chulliyil, R.; Ravi, V. K.; Irfanullah, M.; Chowdhury, A.; Nag, A. Colloidal CsPbBr3 Perovskite Nanocrystals: Luminescence beyond Traditional Quantum Dots. *Angew. Chem. Inte. Ed.* **2015**, 54, 15424-15428.

40. Makarov, N. S.; Guo, S.; Isaienko, O.; Liu, W.; Robel, I.; Klimov, V. I. Spectral and dynamical properties of single excitons, biexcitons, and trions in cesium-lead-halide perovskite quantum dots. *Nano Lett.* **2016**, 16(4), pp 2249-2362

41. Pavitra, E.; Raju, G. S. R.; Park, J. Y.; Wang, L.; Moon, B. K.; Yu, J. S. Novel rare-earth-free yellow Ca5Zn3.92In0.08(V0.99Ta0.01O4)6 phosphors for dazzling white light-emitting diodes. *Sci. Rep.* **2015**, 5, 10296.

42. Krames, M. R.; Shchekin, O. B.; Mueller-Mach, R.; Mueller, G.; Zhou, L.; Harbers, G.; Craford, M. G. Status and Future of High-Power Light-Emitting Diodes for Solid-State Lighting. *J. Display Technol.* **2007**, 3, 160-175.

43. Shannon, C. E. Communication in the Presence of Noise. *Proc. IRE* **1949**, 37, 10-21.

44. Yeh, C. H.; Chow, C. W.; Chen, H. Y.; Chen, J.; Liu, Y. L. Adaptive 84.44−190 Mbit/s phosphor-LED wireless communication utilizing no blue filter at practical transmission distance. *Opt. Express* **2014**, 22, 9783-9788.

45. Khalid, A. M.; Cossu, G.; Corsini, R.; Choudhury, P.; Ciaramella, E. 1-Gb/s Transmission Over a Phosphorescent White LED by Using Rate-Adaptive Discrete Multitone Modulation. *IEEE Photon. J.* **2012**, 4, 1465-1473.

46. Tsonev, D.; Hyunchae, C.; Rajbhandari, S.; McKendry, J. J. D.; Videv, S.; Gu, E.; Haji, M.; Watson, S.; Kelly, A. E.; Faulkner, G.; Dawson, M. D.; Haas, H.; O'Brien, D. A 3-Gb/s Single-LED OFDM-Based Wireless VLC Link Using a Gallium Nitride μLED. *IEEE Photon. Technol. Lett.* **2014**, 26, 637-640.

47. Laurand, N.; Guilhabert, B.; McKendry, J.; Kelly, A. E.; Rae, B.; Massoubre, D.; Gong, Z.; Gu, E.; Henderson, R.; Dawson, M. D. Colloidal quantum dot nanocomposites for visible wavelength conversion of modulated optical signals. *Opt. Mater. Express* **2012**, 2, 250-260.

48. Huang, S.; Li, Z.; Kong, L.; Zhu, N.; Shan, A.; Li, L. Enhancing the Stability of CH3NH3PbBr3 Quantum Dots by Embedding in Silica Spheres Derived from Tetramethyl Orthosilicate in “Waterless” Toluene. *J. Am. Chem. Soc.* **2016**, 138, 5749-5752.

49. de Mello, J. C.; Wittmann, H. F.; Friend, R. H. An improved experimental determination of external photoluminescence quantum efficiency. *Adv. Mater.* **1997**, 9, 230-232.

For Table of Contents Use Only

Perovskite Nanocrystals as a Color Converter for Visible Light Communication

Ibrahim Dursun[1+], Chao Shen[2+], Manas R. Parida[1], Jun Pan[1], Smritakshi P. Sarmah[1], Davide Priante[2], Noktan Alyami[1], Jiakai Liu[1], Makhsud I. Saidaminov[1], Mohd S. Alias[2], Ahmed L. Abdelhady[1], Tien Khee Ng[2], Omar F. Mohammed[1], Boon S. Ooi[2*] and Osman M. Bakr[1*]